Melt Rheology of Lower Critical Solution Temperature Polybutadiene/Polyisoprene Blends

H. S. Jeon,*,† A. I. Nakatani, and C. C. Han

Polymers Division, National Institute of Standards and Technology, Gaithersburg, Maryland 20899

R. H. Colby

Department of Materials Science and Engineering, The Pennsylvania State University, University Park, Pennsylvania 16802

Received April 24, 2000; Revised Manuscript Received July 27, 2000

ABSTRACT: The viscoelastic properties of near critical entangled polybutadiene (PB)/polyisoprene (PI) blends were investigated in oscillatory shear above and below the lower critical solution temperature (LCST). The terminal loss modulus of a near critical PB/PI blend above and below the LCST is well described by means of a log additive mixing rule. A single master curve in the loss modulus of the critical blend exhibiting WLF behavior was obtained above and below the LCST by using the empirical time−temperature superposition (tTS) principle. However, the storage modulus above the LCST deviates from both the tTS principle and the log additive mixing rule. The phase-separated PB/PI blends within the linear viscoelastic regime display higher than expected values of storage modulus at low frequencies, due to the interfacial tension between the two phases of the blend. This increase causes a discontinuity in the temperature dependence of the storage modulus at low frequencies. The discontinuity occurs at a frequency-dependent temperature that extrapolates in the limit of zero frequency to the cloud point measured under quiescent conditions by optical microscopy. The evaluations of interfacial tension from low-frequency linear viscoelasticity are compared with the expectations of Helfand−Tagami theory. The rheological determinations of interfacial tension are within a factor of 2 of the expected values for all compositions except those near the phase-inversion point.

Introduction

The rheology and morphology of viscoelastic polymer blends are of great interest for both scientific and practical industrial reasons. The evolution of domain structure and its response to applied shear are scientifically challenging and important to industry for processing. Viscoelastic polymer blends such as polybutadiene (PB)/polyisoprene (PI) can be homogeneous or heterogeneous depending upon temperature. Rheological properties of multiphase systems are strongly influenced by the morphology, which depends on the thermodynamic interactions between the two constituent polymers and flow history. Rheological properties are therefore essential in order to relate the morphology of the phase-separated state to the processing of multiphase systems.[1,2]

Most experimental work reported in the literature is focused on the rheological properties of immiscible polymer blends obtained from oscillatory or steady shear flow,[3−8] in which pronounced elastic properties and very long relaxation times are typically observed. On the other hand, the effect of phase separation on the linear viscoelastic properties of miscible polymer blends has only recently become a topic of interest.[9,10] In the single phase state of blends with closely matched component glass transition temperatures, the time−temperature superposition (tTS) principle can be applied to both the dynamic storage modulus (G') and the loss modulus (G'').[11]

We report the viscoelastic properties of entangled PB/PI blends with $\Delta T_g \approx 27$ K above and below the lower critical solution temperature (LCST) measured by oscillatory shear rheology. The linear viscoelastic response of the phase-separated PB/PI blends displays high values of the storage modulus at low frequencies. This is due to the interfacial tension between the two phases of the blends, modeled here using the analyses of Gramespacher and Meissner[6] derived from a theory for mixtures of Newtonian liquids developed by Choi and Schowalter[13] and Palierne for the viscoelastic emulsions of incompressible materials.[12]

The dynamic modulus of immiscible polymer blends may depend on the domain size and/or concentration of the dispersed phase. These effects have been previously reported for immiscible blends of polystyrene (PS)/poly(methyl methacrylate) (PMMA)[6,14] and polyisobutene (PIB)/poly(dimethylsiloxane) (PDMS).[8] Jeon et al. showed the quantitative effect of droplet size on the storage and loss moduli of the phase-separated PB/PI blends.[15] An increase in the concentration of PI or domain size of the blends caused increases in G' and G'' of the PB/PI blends. To study the effects of domain deformation on the dynamic modulus, we measured G' and G'' at two different perturbation conditions: small strain amplitude ($\gamma_0 = 0.08$) and large strain amplitudes ($\gamma_0 > 6.0$ at low frequencies). The large strain amplitudes at low frequencies strongly affected G', whereas G'' was relatively independent of strain amplitude.

Experimental Section

The polymers used in this study were supplied by The Goodyear Tire and Rubber Company.[16] The number-average molecular weight (M_n), the mass-average molecular weight

† Current address: Department of Petroleum and Chemical Engineering, New Mexico Institute of Mining and Technology, 801 Leroy Place, Socorro, NM 87801.

* To whom correspondence should be addressed.

10.1021/ma000714u CCC: $19.00
Published on Web 12/02/2000

Table 1. Characterization Data of Polymers

sample code	M_n (g/mol)	M_w/M_n	η_0 (Pa·s)[a]	T_g (°C)	microstructure, mol %			
					cis-1,4	*trans*-1,4	1,2	3,4
PB	51 000	1.03	220 ± 0.3	−93	44	47	9	0
PI	88 000	1.08	700 ± 0.7	−66	74	14	0	12

Table 2. Parameters Used in Gramespacher and Meissner's Analysis and Interfacial Tension at 130 °C

blends	ϕ_{PI}	R_n[b] (μm)	R_v[b] (μm)	R_v/R_n	η_0[a] (Pa·s)	R/σ (m^2/N)	σ_n (mN/m)	σ_v (mN/m)
D10	0.102	1.9 ± 0.1[c]	2.2	1.12	256 ± 1.0	0.008	0.24	0.27
D20	0.204	4.5 ± 0.2	5.0	1.10	315 ± 0.4	0.010	0.45	0.50
D30	0.306	9.0 ± 0.6	11.9	1.31	355 ± 1.2	0.012	0.75	0.99
D40	0.408	11.5 ± 1.0	18.7	1.63	391 ± 0.8	0.017	0.68	1.10
D50	0.500	11.8 ± 1.0	17.9	1.52	431 ± 1.2	0.010	1.20	1.79
D60	0.602	13.7 ± 0.9	19.0	1.39	454 ± 2.6	0.0045	3.00	4.22
D70	0.714	9.0 ± 0.6	11.2	1.25	484 ± 3.1	0.0035	2.20	3.21
D80	0.816	3.3 ± 0.1	3.6	1.08	530 ± 3.0	0.0030	1.10	1.19

[a] The dynamic zero shear viscosity of homopolymers and blends was obtained by averaging over plateau values of viscosity at a wide range of frequency at 130 °C. [b] The average radius of dispersed droplet was obtained by examining a full micrograph (220 × 160 μm^2) and averaging 23−58 droplets per sample. [c] The uncertainties in quoted numerical results represent the estimate of the standard error in experimental uncertainty. [d] The subscript n refers to number-average particle size, and the subscript v refers to volume-average particle size.

(M_w), and the polydispersity of model polymers were determined by gel permeation chromatography (Waters model 150-C).[16,17] The composition of these materials was obtained by ^{13}C NMR. The results of the polymer characterization are summarized in Table 1. The polybutadiene (PB)/polyisprene (PI) blends were prepared by solution blending.[15] The exact compositions and designation of blends used in this study are given in Table 2. The PB/PI blends are labeled as D_{xx}, where *xx* is the volume percent of PI in the blends. We started with a dilute solution in methylene chloride (mass fraction of 2% total polymer) containing the appropriate amount of each component and about 0.05% Goodyear Wingstay #29[16] as an antioxidant. The mixture was stirred at room temperature for 1 day and filtered through a 0.45 μm PTFE filter. The solvent was evaporated under flowing nitrogen gas, and the sample was dried in a vacuum oven at room temperature for several days before doing the experiments. The phase separation temperature and morphology of the blend were determined by phase contrast optical microscopy.[18] Normal bright field microscopy requires a refractive index difference in the sample to resolve the image. In the case of the phase-separated PB/PI blend, it is difficult to obtain a clear image with the normal bright field microscope because the refractive index difference between these two components is very small ($n_{PB} = 1.512$ and $n_{PI} = 1.517$).[19] A near critical PB/PI blend (D40) has a lower critical solution temperature (LCST) of 61.5 ± 0.5 °C; hence, the blend is a single phase at low temperatures (<61.5 °C) and phase-separated at elevated temperatures (>61.5 °C). The prepared samples were heated from room temperature to the desired experimental temperature in the two-phase region and then held for 120 min to obtain a reproducible two-phase morphology for each sample without preshearing. The droplet deformation of the phase-separated PB/PI blends under simple shear flow was measured by in situ shear light scattering microscope instrument. The microscope image was collected with a CCD camera (Dage MTI, model 72), recorded onto a super-VHS tape, and digitized using a frame grabber from Data Translation (DT 3851). The geometry of the instrument is such that it probes structures within the plane defined by the flow and neutral directions. A detailed description is given elsewhere.[18]

A Rheometric Scientific SR-5000 controlled-stress rheometer[16] was utilized in the parallel-plate geometry for oscillatory shear measurements. Our measurements were carried out with 25 mm diameter fixtures and 0.4 ± 0.01 mm gap thickness. The temperature was controlled by electrically heated top and bottom plates to within ±0.1 °C. The measurements were carried out under nitrogen atmosphere to minimize thermal degradation of the polymers which are known to be extremely sensitive to heat. To study the linear viscoelastic properties at low frequencies, the oscillatory shear measurements were performed in a constant strain mode with a small strain amplitude ($\gamma_0 = 0.08$). The oscillatory shear measurements were also performed in constant stress mode with a large stress to produce a large deformation of droplets at low frequencies. We should note that all the rheological data shown in this paper without specific comments were measured under the small strain amplitude ($\gamma_0 = 0.08$) conditions.

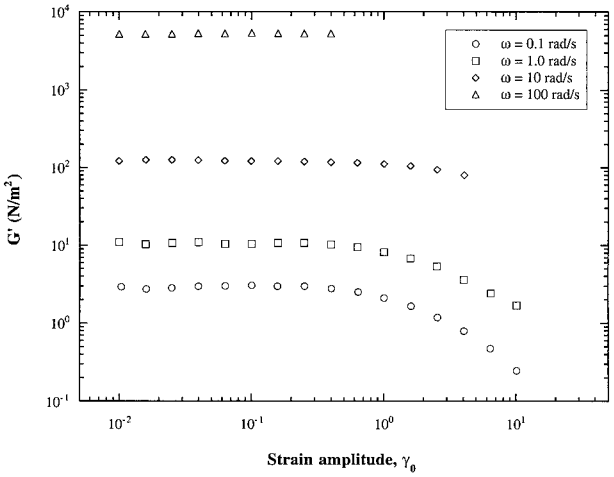

Figure 1. Typical linear viscoelastic behavior of a phase-separated PB/PI blend, D40, for various frequencies (0.1, 1.0, 10, and 100 rad/s) at 130 °C.

Results and Discussion

Limit of Linear Viscoelasticity. At small strain amplitudes, the measurements are carried out with minimal deformation of sample morphology. If the strain amplitude is sufficiently small, the ratio of stress to strain is only a function of time because the morphology slowly evolves with time. To determine the limits of linear viscoelasticity, we performed a dynamic strain sweep at 130 °C for a range of frequencies (0.1−100 rad/s) as shown in Figure 1. The linear viscoelastic response is evident from the constant values of G' as a function of strain up to $\gamma_0 = 0.4$ at all frequencies. Therefore, the applied strain amplitude ($\gamma_0 = 0.08$) was within the linear viscoelastic regime.

Time−Temperature Superposition (tTS). A frequency shift factor, $a_T = \eta_0(T)/\eta_0(T_0)$, can be calculated directly from the dynamic viscosity data since the temperature dependence of viscosity depends directly

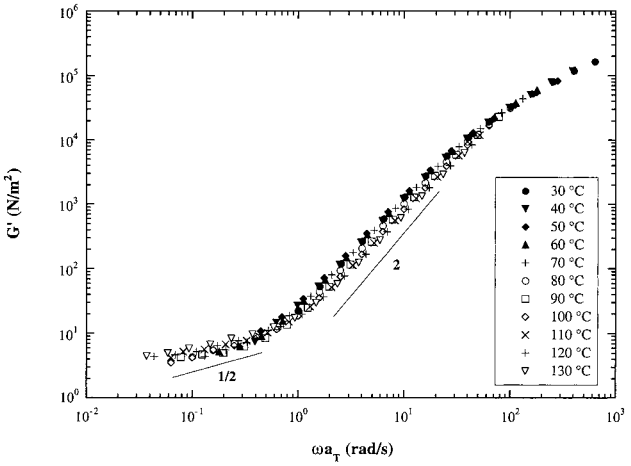

Figure 2. A reduced frequency plot of dynamic storage modulus, G', for a near critical PB/PI blend, D40, at various temperatures (30−130 °C) which cover the single-phase and two-phase regions in the PB/PI phase diagram (see an inset of Figure 10): single-phase (solid symbols), two-phase (open symbols). A single master curve was only obtained for the single-phase temperatures of a D40 blend by using a time−temperature superposition (tTS) principle.

on a_T. The WLF equation given by eq 1 describes rather well the temperature dependence of a_T for most polymer melts and concentrated solutions.[20] The values for the parameters $C_1 = 1.83$ and $C_2 = 163$ K of eq 1 were obtained from a nonlinear least-squares fitting of the η_0 data from the D40 blend using a reference temperature, $T_0 = 80$ °C.

$$\log a_T = \frac{-C_1(T - T_0)}{C_2 + (T - T_0)} \tag{1}$$

For a monodisperse polymer in the terminal region $G' \propto \omega^2$ and $G'' \propto \omega$. The same behavior is also exhibited by homogeneous blends of monodisperse homopolymers.[20] If the blends are phase-separated, the values of G' and G'' increase, and the exponents of G' vs ω and G'' vs ω are typically less than 2.0 and 1.0 in the terminal regime, respectively. Typically, phase separation in a polymer blend occurs by changing temperature. In the single-phase region, the storage and loss moduli of the PB/PI blends were found to obey the time−temperature superposition (tTS) principle applying the same shift factors (see eq 1) obtained from the zero-shear viscosity:

$$G'(\omega,T) = G'(a_T\omega,T_0) \tag{2}$$

$$G''(\omega,T) = G''(a_T\omega,T_0) \tag{3}$$

Figure 2 shows a master curve of the storage modulus for D40 blend at various temperatures, which covers both the single-phase and two-phase regions in the phase diagram. The tTS principle applied well for temperatures in the homogeneous regime ($T < 61.5$ °C, filled symbols). On the other hand, the tTS principle failed for temperatures in the two-phase region, where G' (open symbols) does not collapse onto a single master curve. There have been several reports about the deviation from the tTS principle in the phase-separated state[10] or single-phase blend.[21] In the intermediate reduced frequency regime (1 rad/s $< \omega a_T <$ 100 rad/s), the slope of G' is close to 2, similar to the characteristic

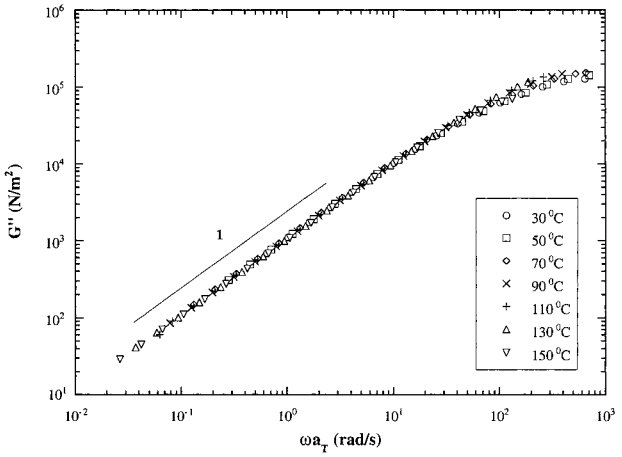

Figure 3. A reduced frequency plot of dynamic loss modulus, G'', for a near critical PB/PI blend (D40) at various temperatures which cover the single-phase and two-phase regions in the PB/PI phase diagram (see an inset of Figure 10). A single master curve of the loss modulus above and below the lower critical solution temperature (LCST) for a D40 blend was obtained by using a time−temperature superposition (tTS) principle.

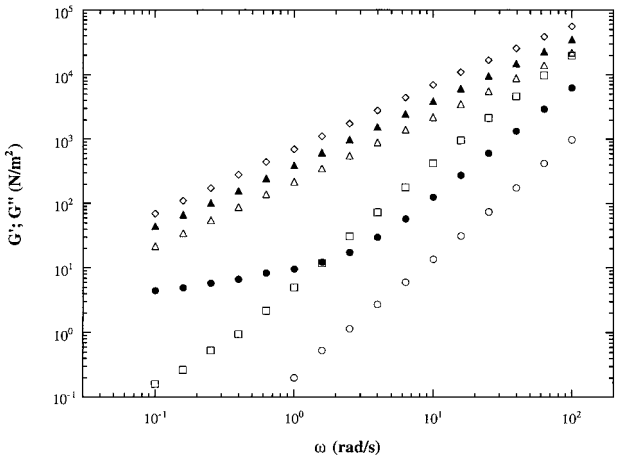

Figure 4. Dynamic storage modulus (G') and loss modulus (G'') as a function of frequency at 130 °C. Storage modulus: PB (open circles); PI (open squares); D40 blend (closed circles). Loss modulus: PB (open triangles); PI (open diamonds); D40 blend (closed triangles).

behavior of a monodisperse polymer in the terminal regime. In the terminal regime, the storage modulus is larger than the extrapolation based on ω^2. The slope of log G' vs log ωa_T is less than 2 and close to 0.5. The experimental values of the terminal regime exponents for G' obtained from other two-phase polymer blends vary between 0.5 and 1.0[10].

Figure 3 shows the loss modulus master curve of the D40 blend. In contrast to the storage modulus, a single master curve of G'' for the blend is obtained, which shows no anomalous terminal response, even deep into the two-phase region. The loss modulus has been shown to be either insensitive[22] or very weakly sensitive[11,23] to phase separation in other polymer blends.

Effects of Domain Size and Interfacial Tension. Figure 4 shows the storage and loss moduli for the homopolymers (PB and PI) and the phase-separated D40 blend at 130 °C. At high frequencies ($\omega > 1$ rad/s), the values of the storage modulus for the blend lie between the storage moduli of the homopolymers. However, at low frequencies (<1 rad/s), the storage

modulus of the blend shows a large deviation from the log additive mixing rule.[2] The deviation is characterized by an emergence of a pronounced storage modulus at low frequencies, presumably caused by the interfacial tension. In contrast, the loss modulus of the blend lies between the loss modulus values for the homopolymers over the entire frequency range.

For the description of the influence of the interfacial tension on the storage and loss moduli, we use the equations of Gramespacher and Meissner (G−M)[6] derived from a theory for mixtures of Newtonian liquids developed by Choi and Schowalter.[13] They attribute any deviation of the complex modulus of the blend from a simple linear addition of the components to interfacial tension.

$$G'_{\text{blend}} = G'_{\text{components}} + G'_{\text{interface}}$$

$$= (\phi_A G'_A + \phi_B G'_B) + \frac{\eta}{\tau_1}\left(1 - \frac{\tau_2}{\tau_1}\right)\frac{\omega^2 {\tau_1}^2}{1 + \omega^2 {\tau_2}^2} \quad (4)$$

$$G''_{\text{blend}} = G''_{\text{components}} + G''_{\text{interface}}$$

$$= (\phi_A G''_A + \phi_B G''_B) + \frac{\eta}{\tau_1}\left(1 - \frac{\tau_2}{\tau_1}\right)\frac{\omega \tau_1}{1 + \omega^2 {\tau_1}^2} \quad (5)$$

The volume fractions of the components are ϕ_A and ϕ_B, with the subscript A denoting the dispersed phase. In the above equations, the parameters τ_1 and τ_2 are calculated from

$$\tau_1 = \tau_0\left[1 + \phi_A \frac{5(19\lambda + 16)}{4(\lambda + 1)(2\lambda + 3)}\right] \quad (6)$$

$$\tau_2 = \tau_0\left[1 + \phi_A \frac{3(19\lambda + 16)}{4(\lambda + 1)(2\lambda + 3)}\right] \quad (7)$$

$$\tau_0 = \frac{\eta_m R}{\sigma} \frac{(19\lambda + 16)(2\lambda + 3)}{40(\lambda + 1)} \quad (8)$$

$$\lambda = \frac{\eta_d}{\eta_m} \quad (9)$$

In these equations, η_d and η_m are the Newtonian viscosity of the dispersed phase and matrix phase of the mixture, respectively, λ is the viscosity ratio, R is the radius of dispersed droplets, and σ is the interfacial tension. For the application of these equations to our phase-separated PB/PI blends, the following assumptions were made: (1) The viscosity of the PB-rich (or PI-rich) matrix phase is equal to the viscosity of the PB/PI blend with PB-rich (or PI-rich) continuous phase having the equilibrium composition of the PB/PI phase diagram at each temperature. (2) The droplet radius used in each calculation is equal to the volume-averaged radius of the dispersed droplets.

The assumption (1) is very reasonable because our phase-separated blends correspond to a near equilibrium state. The binodal curve for PB/PI blends was measured with phase contrast optical microscopy[15] and is shown in the inset of Figure 10. The equilibrium compositions at a given temperature can be predicted from the least-squares fit through the cloud points of the PB/PI phase diagram.[24] We used a fourth-order polynomial equation for the prediction of the compositional dependence of T_C in the PB/PI phase

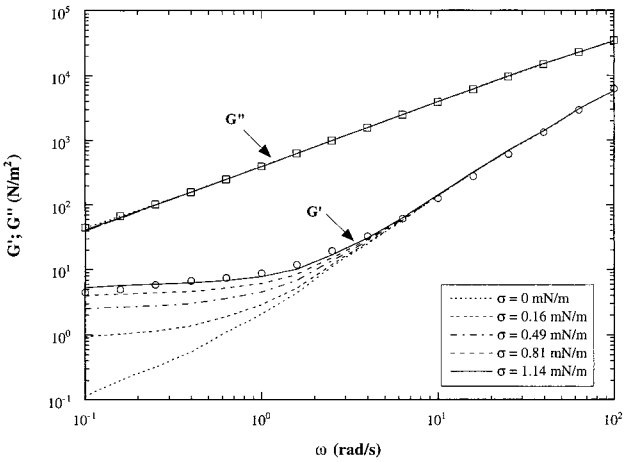

Figure 5. Effect of interfacial tension on the calculated dynamic storage and loss moduli (solid and dashed curves) for given values of the volume fraction ($\phi_{PI} = 0.4$) and the volume average radius ($R = 18.7$ μm) of the dispersed droplets at 130 °C. Measured storage modulus (open circles) and loss modulus (open squares) for D40 blend at 130 °C. The calculated G' and G'' values of the blend are represented with the different values ($\sigma = 0-1.14$ mN/m) of interfacial tension. The droplet radius of dispersed phase used in the calculations of G' and G'' was independently measured under quiescent conditions by using optical microscopy.

diagram. The solid curve is the fit for a polynomial equation through the experimental data (see inset of Figure 10). The resulting equation is $T_C = 143 - 605\phi_{PI} + 1743{\phi_{PI}}^2 - 2327{\phi_{PI}}^3 + 1237{\phi_{PI}}^4$. The equilibrium compositions obtained from the nontrivial solutions of ϕ_{PI} from the previous equation are 0.023 and 0.909 at $T_C = 130$ °C. Therefore, we estimated η_d from the viscosity of PB/PI blend with $\phi_{PI} = 0.023$ and η_m from the viscosity of a PB/PI blend with $\phi_{PI} = 0.909$ using the log additive mixing rule. In all cases we used the measured viscosity η of the blends.

Figure 5 shows the effect of interfacial tension on the calculated storage modulus (G') and loss modulus (G'') of the D40 blend for a given volume fraction ($\phi_{PI} = 0.4$) and volume average radius ($R = 18.7$ μm) of the dispersed droplets based on the model eqs 4−9, with the assumptions discussed previously. Since the volume fraction, droplet radius, and viscosity are all known, the only adjustable parameter for the results shown in Figure 5 is the interfacial tension, σ (see Table 2). The curves calculated from the model equations as a function of interfacial tension represent the effect of domain interfaces on G' and G''. At high frequencies ($\omega > 10$ rad/s), it is evident that the storage modulus is not affected by the interfacial tension, whereas the storage modulus at lower frequencies ($\omega < 10$ rad/s) is sensitive to the interfacial tension value. In contrast, the loss modulus of the blend is not affected significantly by the interfacial tension and is identical with the predictions from the additive mixing rule of matrix and dispersed components. Therefore, it is clear that the high values of G' at low frequencies can be explained quantitatively by the contribution of the interfacial energy of the phase-separated blend from eq 4. For a fixed volume fraction, if the interfacial tension increases or the droplet size decreases, the pronounced elasticity at low frequencies is predicted to increase.

Figure 6a shows the effect of PI concentration on the storage modulus (G') of the PB/PI blends at 130 °C. The curves in Figure 6a represent the calculated G' based

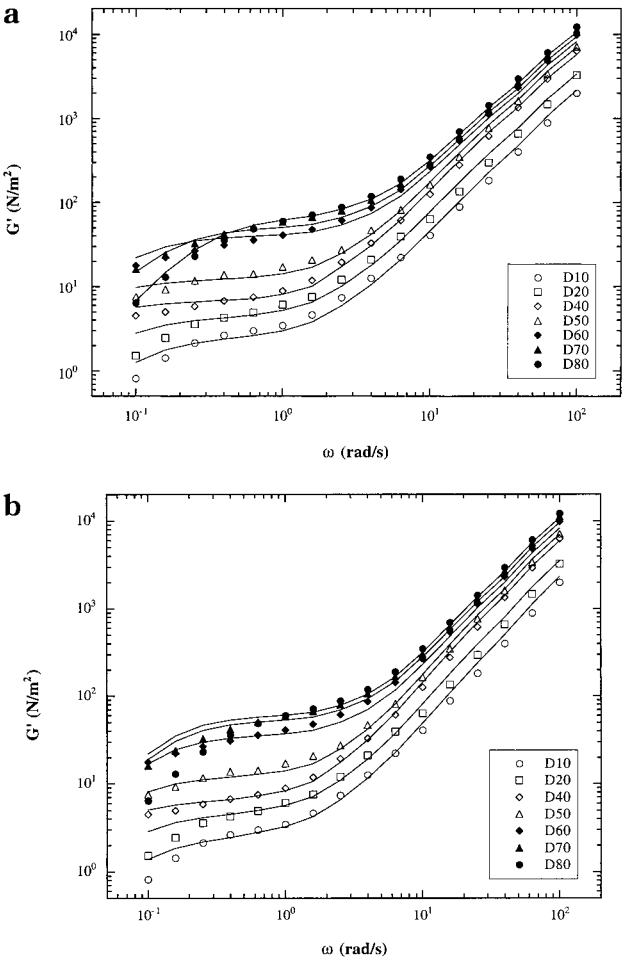

Figure 6. (a) Dynamic storage modulus from the phase-separated PB/PI blends at 130 °C: D10 (open circles); D20 (open squares); D40 (open diamonds); D50 (open triangles); D60 (filled diamonds); D70 (filled triangles); D80 (filled circles). The solid curve through the data represents the calculated G' from the Gramespacher and Meissner model. (b) Dynamic storage modulus from the phase-separated PB/PI blends at 130 °C: D10 (open circles); D20 (open squares); D40 (open diamonds); D50 (open triangles); D60 (filled diamonds); D70 (filled triangles); D80 (filled circles). The solid curve through the data is the predicted G' from the Palierne model.

on the G−M model eqs 4−9. For the comparison between the experimental and calculated values of the storage modulus, the interfacial tension has been determined empirically so that the model function fits the experimental values of G' for the low and high frequencies. A good overall agreement is observed between experimental results and predictions of the model. The experimentally measured parameters (R and η_0) that are used in these calculations and the interfacial tension determined from the fitting are summarized in Table 2. It is clear that there is well-developed dependence of G' on PI concentration until $\phi_{PI} = 0.6$ (D60). However, the storage moduli of the D70 and D80 blends at low frequencies ($\omega < 0.4$ rad/s) show significant deviations and do not depend on the concentration of PI. This is due to the decrease in the droplet radius of the dispersed phase when the concentration of PI in the blends increases from $\phi_{PI} = 0.6$ to $\phi_{PI} = 0.7$ and $\phi_{PI} = 0.8$. It is also interesting to note that the theoretical predictions overestimate the storage modulus, G', at low frequencies ($\omega < 0.2$ rad/s). This may be explained by polydispersity (see Table 2) of the dispersed domains in the PB/PI blends. At lower frequencies or longer relaxation times, relatively large droplets dominate the storage modulus. At a fixed concentration of PI, the predicted value of G' increases as the droplet radius decreases or interfacial tension increases.

Alternatively, we can use the Palierne analysis for the viscoelastic emulsions of incompressible materials in the linear viscoelastic range of deformation to determine the interfacial tension,[12] where the dispersed droplets are assumed to be spherical and of equilibrium composition. If the complex, frequency-dependent surface dilation modulus, surface shear modulus, and the polydispersity of dispersed droplets are assumed to be negligible, the following simplified expression for the complex modulus of a blend is obtained:

$$G^* = G^*_m(\omega)\frac{1 + 3\phi H(\omega)}{1 - 2\phi H(\omega)} \tag{10a}$$

with

$$H(\omega) = \frac{4\frac{\sigma}{R}[2G^*_m(\omega) + 5G^*_d(\omega)] + [G^*_d(\omega) - G^*_m(\omega)][16G^*_m(\omega) + 19G^*_d(\omega)]}{40\frac{\sigma}{R}[G^*_m(\omega) + G^*_d(\omega)] + [3G^*_m(\omega) + 2G^*_d(\omega)][16G^*_m(\omega) + 19G^*_d(\omega)]} \tag{10b}$$

where $G^*_m(\omega)$ and $G^*_d(\omega)$ are the complex modulus of the matrix and dispersed phases at frequency ω, respectively, and ϕ is the volume fraction of dispersed phase component. For simplicity, if we assume that the interfacial tension is constant in a mixture of two Newtonian liquids, the model equation can be simplified as

$$G^*(\omega) = i\omega\eta\frac{1 + i\omega\tau_2}{1 + i\omega\tau_1} \tag{11}$$

In the above equations, the parameters τ_1 and τ_2 are calculated from

$$\tau_1 = (0.25R\eta_m/\sigma)\frac{(19\lambda + 16)[2\lambda + 3 - 2\phi_A(\lambda - 1)]}{10(\lambda + 1) - 2\phi_A(5\lambda + 2)} \tag{12}$$

$$\tau_2 = (0.25R\eta_m/\sigma)\frac{(19\lambda + 16)[2\lambda + 3 - 3\phi_A(\lambda - 1)]}{10(\lambda + 1) + 3\phi_A(5\lambda + 2)} \tag{13}$$

In these equations, η_m is the Newtonian viscosity of the matrix phase of the mixture, λ is the viscosity ratio, R is the radius of dispersed droplets, and σ is the interfacial tension. Since our polymer blends are viscoelastic liquids, the assumption of Newtonian fluids used in our Palierne analysis is only valid at low frequencies, where $G' \ll G''$. Therefore, to account for the frequency dependence of the blend over the whole frequency range, we use a simple additive mixing rule and write for our PB/PI blends:[5]

$$G'_{blend} = (\phi_A G'_A + \phi_B G'_B) + \frac{\omega^2\eta(\tau_1 - \tau_2)}{1 + \omega^2\tau_1^2} \tag{14}$$

$$G''_{blend} = (\phi_A G''_A + \phi_B G''_B) + \frac{\omega^2\eta(1 + \omega^2\tau_1\tau_2)}{1 + \omega^2\tau_1^2} \tag{15}$$

Table 3. Parameters Used in Palierne's Analysis and Interfacial Tension at 130 °C

blends	ϕ_{PI}	R_n[b] (μm)	R_v[b] (μm)	R_v/R_n	η_0[a] (Pa·s)	R/σ (m^2/N)	σ_n (mN/m)	σ_v (mN/m)
D10	0.102	1.9 ± 0.1[c]	2.2	1.12	256 ± 1.0	0.013	0.15	0.17
D20	0.204	4.5 ± 0.2	5.0	1.10	315 ± 0.4	0.014	0.32	0.36
D30	0.306	9.0 ± 0.6	11.9	1.31	355 ± 1.2	0.016	0.56	0.74
D40	0.408	11.5 ± 1.0	18.7	1.63	391 ± 0.8	0.019	0.61	0.98
D50	0.500	11.8 ± 1.0	17.9	1.52	431 ± 1.2	0.012	0.98	1.49
D60	0.602	13.7 ± 0.9	19.0	1.39	454 ± 2.6	0.0054	2.54	3.52
D70	0.714	9.0 ± 0.6	11.2	1.25	484 ± 3.1	0.0037	2.42	3.03
D80	0.816	3.3 ± 0.1	3.6	1.08	530 ± 3.0	0.0033	1.01	1.08

[a] The dynamic zero shear viscosity of homopolymers and blends was obtained by averaging over plateau values of viscosity at a wide range of frequency at 130 °C. [b] The average radius of dispersed droplet was obtained by examining a full micrograph (220 × 160 μm^2) and averaging 23−58 droplets per sample. [c] The uncertainties in quoted numerical results represent the estimate of the standard error in experimental uncertainty. [d] The subscript n refers to number-average particle size, and the subscript v refers to volume-average particle size.

The curves in Figure 6b represent the predicted G' from the Palierne model for emulsions of two Newtonian liquids[5] and the additive mixing rule. For comparison between the experimental and predicted values of G', the interfacial tension was determined by trial and error to obtain the best fit to the experimental values of $G'(\omega)$ for the low and high frequencies. A good overall agreement between experimental and theoretical curves is obtained over the whole frequency range. The experimentally measured parameters (R and η) that are needed to calculate G' and G'' in the Palierne model and the interfacial tension determined from the fitting are summarized in Table 3. The Palierne analysis of G' provides slightly better agreement with data than the analysis of the G−M at low frequencies (ω < 0.2 rad/s) for D40, D50, and D60.

As a third approach, we determined the interfacial tension from the D40 and D60 blends by measuring the aspect ratios of dispersed domains under simple shear flow.[25] To determine the interfacial tension, we use Taylor theory for a single droplet,[26] which gives the following relation:

$$D = \frac{2(1 + 1.1875\lambda)}{1 + \lambda} Ca \qquad (16)$$

where $D = (\zeta - 1)/(\zeta + 1)$ is the deformation factor, where ζ is the aspect ratio of deformed domains under simple shear, and $Ca = \eta\dot{\gamma}R/\sigma$, where Ca is the Capillary number, η is the viscosity of continuous phase, $\dot{\gamma}$ is the shear rate, R is the radius of droplet, and σ is the interfacial tension. Equation 16 only holds for the deformation of a droplet under simple shear flow without breakup. Taylor theory suggests that droplet breakup occurs when Ca > 1. In the D40 blend with λ = 3.2, the breakup was observed at $Ca \approx 0.2$, whereas the breakup was not observed until $Ca \approx 2.0$ in D60 blend with λ = 0.3. The interfacial tensions obtained from the linear plots of D vs $\dot{\gamma}$ based on eq 16 in D40 and D60 blends are 0.35 and 0.33 mN/m, respectively.

As a fourth approach, we predicted the interfacial tension of the PB/PI blend from the Helfand−Tagami (H−T) theory extended by Broseta et al.,[27] which requires the Flory−Huggins interaction parameter (χ), the statistical segment length (b), the monomer density (ρ_0), and the molecular weight to predict the interfacial tension σ.

$$\sigma = b\rho_0 kT(\chi/6)^{1/2}\left[1 - \frac{\pi^2}{12\chi}\left(\frac{1}{N_A} + \frac{1}{N_B}\right)\right] \qquad (17)$$

N_A and N_B are the degree of polymerization of polymers A and B, respectively, k is the Boltzmann constant, and T is the absolute temperature. The parameters that are needed to calculate the interfacial tension of the PB/PI blend are obtained from small-angle neutron scattering.[28] The interfacial tension of the PB/PI blend predicted from the eq 17 was 0.676 mN/m. The numerical values of the parameters that are needed to calculate this estimate of the interfacial tension of the PB/PI blend at 130 °C were given in ref 29.

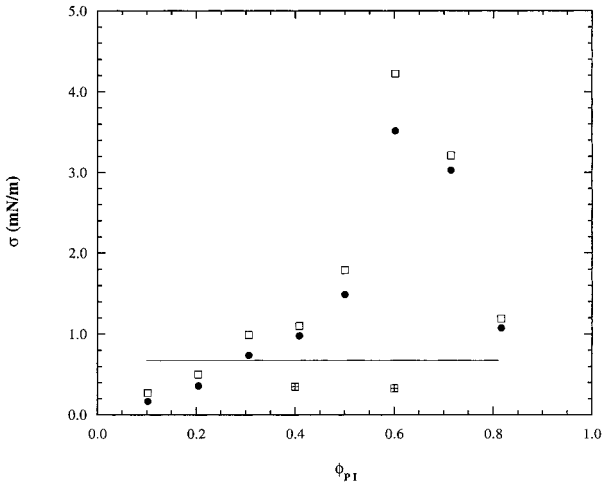

Figure 7. Interfacial tensions estimated by various methods for different blend compositions at 130 °C. The solid line represents the interfacial tension predicted from the Helfand−Tagami theory, which does not change at the phase inversion point. Symbols: Taylor theory (hatched squares); Palierne model (filled circles); Gramspacher−Meisner model (open squares).

Figure 7 compares the interfacial tensions estimated by various methods for different blend compositions at 130 °C. The interfacial tension of the blends increases smoothly as the PI volume fraction increases from 0.1 to 0.5 due to the increase in the storage modulus of the blends. A large increase in the interfacial tension occurs at ϕ_{PI} = 0.55, which corresponds to the phase inversion composition determined from the storage modulus.[15] The model of Utracki[30] predicts the phase inversion composition of our PB/PI blend, 0.6, in good agreement with our experimental value. The solid line in Figure 8 represents the interfacial tension predicted from the H−T theory, which does not change at the phase inversion point. The dramatic increases of the interfacial tension from both the Palierne and G−M's analyses around the phase inversion composition suggest that the rheological methods for determining the interfacial tension of polymer melt blends have some sort of crisis near the phase inversion point. That crisis could be caused by co-continuous structures being formed, but

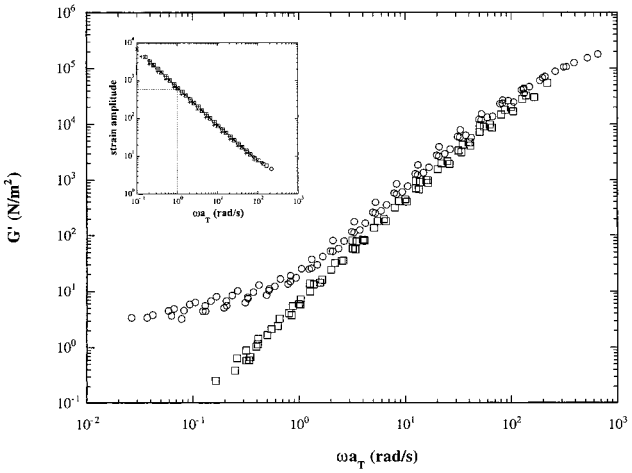

Figure 8. Storage modulus of D40 blend measured under the two different perturbation conditions: (1) constant strain amplitude ($\gamma_0 = 8.08$, circles) and (2) constant stress (5000 N/m^2, squares). Oscillatory shear measurements were performed at constant-stress mode with a large stress, which gives large strains, $\gamma_0 \geq 6.0$, at the low frequencies ($\omega a_T \leq 1.0$ rad/s) (see an inset of Figure 8). Inset: a reduced frequency plot of strain amplitude D40 blend at various temperatures (30−130 °C) which covers the single-phase and two-phase regions in the phase diagram.

our microscopy results on all PB/PI blends studied show only discrete droplets. However, there is a possibility of complex morphologies around phase inversion point. Recently, Grizzuti et al. reported that they observed a much more complex morphology from an immiscible polyisobutylene (PIB)/poly(dimethylsiloxane) (PDMS) blend, made of repeatedly nested droplets instead of co-continuous structures near the phase inversion point.[31] We perhaps missed PI-rich droplets within the large PB-rich droplets (or vice versa) near the phase inversion point due to the relatively very small refractive index contrast of our PB/PI blends than that of PIB/PDMS blend.

Effects of Domain Deformation on G' and G''. To study the effect of domain shapes on the dynamic modulus, we measured G' and G'' at two different perturbation conditions: (1) constant strain amplitude ($\gamma_0 = 0.08$) and (2) constant stress (5000 N/m^2). Figure 8 shows the storage modulus of D40 blend measured under the two different shear conditions. At $\gamma_0 = 0.08$, we find a large deviation in G' at low ω due to the increase in interfacial tension described above, whereas at constant stress no deviation in G' from interfacial tension at low ω is observed. The domain deformation under these two conditions is extremely different. The small constant strain amplitude does not substantially alter the droplet shape of the dispersed phase and yields a linear viscoelastic response. The large constant stress produces much larger strain amplitudes ($\gamma_0 > 6.0$) at low frequencies ($\omega a_T < 1$) (see the inset of Figure 8). The high stress or large strain amplitude at low frequencies elongates the dispersed domains, resulting in stringlike domains, and eventually can result in a shear-induced mixing or homogenization.[32] We repeated the linear viscoelasticity experiments to confirm the possibility of sample instability or droplet aggregation after large stress amplitude experiment. However, the linear viscoelastic response was maintained after the large strain amplitude experiment. Apparently, domain elongation at large strain amplitudes ($\gamma_0 > 6.0$) destroys most of the additional contribution by the interfacial tension to G' at low frequencies, resulting in typical terminal zone behavior being observed over all frequencies for G'.

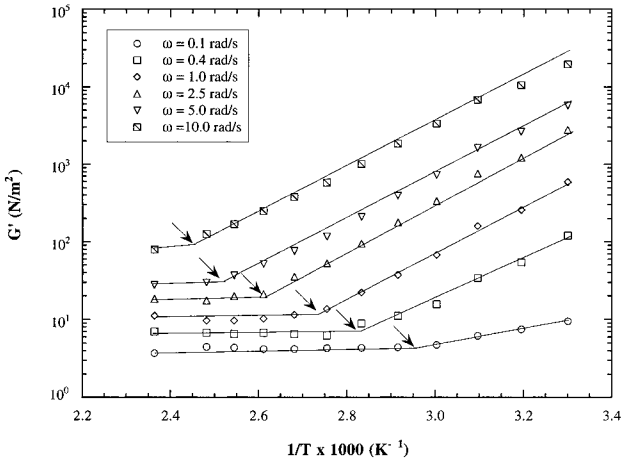

Figure 9. Dependencies of G' on temperature at different frequencies (ω = 0.1, 0.4, 1.0, 2.5, 5.0, and 10 rad/s) for D40 blend. The arrows indicate the apparent phase-separation temperature of the blend at each frequency.

Rheological Determination of Phase Separation Temperature. As the phase separation temperature is approached, the linear viscoelastic properties of the blend change substantially. Oscillatory shear experiments at various temperatures above and below the LCST were carried out at a fixed strain amplitude ($\gamma_0 = 0.08$) corresponding to linear response. The purpose of this experiment is to determine the temperature dependence of the linear viscoelastic properties of the blend in the vicinity of phase separation. Figure 9 shows the temperature dependence of storage modulus at different frequencies (ω = 0.1, 0.4, 1.0, 2.5, 5.0, and 10 rad/s) for the near critical blend D40. It is clear that there are discontinuities in the slope of log G' vs T^{-1} that occur at different temperatures for different frequencies. In the homogeneous regime, an increase in temperature results in a decrease of G' due to the increase of chain mobility. The homogeneous mixture has WLF dependence on temperature, which is typical for single-phase polymer systems in the terminal viscoelastic regime. As the temperature increases further into the two-phase region, however, the storage modulus at low frequencies (ω < 10 rad/s) is dominated by the interfacial tension between the droplets and the matrix, and the interfacial tension has only a weak temperature dependence. Using the above information, we assign the point of change in the slope of log G' vs T^{-1} plot to the apparent phase separation temperature $T_X(\omega)$ indicated by arrows.

Figure 10 shows the frequency dependence of the apparent phase separation temperature $T_X(\omega)$ obtained from a near critical PB/PI blend (D40) data of Figure 10. Decreasing the frequency from 10 to 0.1 rad/s results in a continuous decrease in the apparent phase separation temperature $T_X(\omega)$. The inset of Figure 10 represents the LCST phase diagram of PB/PI blend. The solid curve in the inset of Figure 10 is the least-squares fit with the polynomial equation through the experimental data obtained from D40 blend, and the dashed curve is the extrapolation from the polynomial equation fit of $T_X(\omega)$. An extrapolation to $\omega = 0$ gives the phase separation temperature, $T_C = 61.5 \pm 0.5$ °C (see inset of Figure 10).

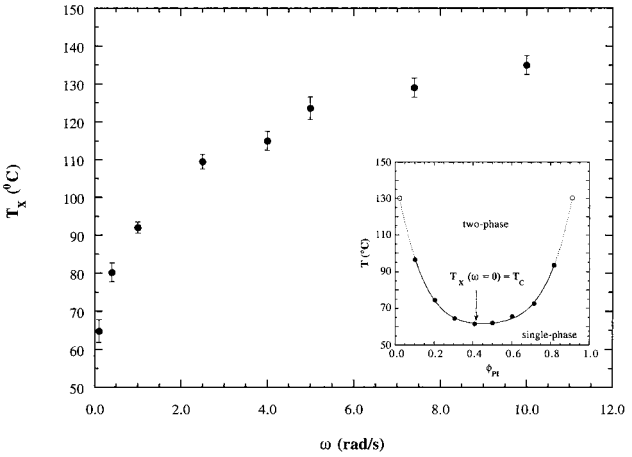

Figure 10. Frequency dependence of the apparent phase-separation temperature, $T_X(\omega)$. $T_X(\omega)$ was obtained from the D40 blend. The bars show the error range of $T_X(\omega)$ values determined from G' measurement as a function of temperature from the blend in both single-phase as well as phase separated regimes. Inset: the lower critical solution temperature (LCST) phase diagram as a function of PI concentration (ϕ_{PI}) for the PB/PI blends. The filled circles represent phase separation temperatures of PB/PI blends measured from optical microscopy, and the open circles represent the predicted phase separation temperature from the experimental data. The solid curve is the least-squares fit for a polynomial equation through the experimental data. The dashed curves represent the predictions of the phase transition temperature of PB/PI blends from the polynomial equation.

Conclusions

Phase-separated PB/PI blends have large values of their linear viscoelastic storage modulus at low frequencies. This is due to interfacial tension between the two phases, and the interfacial tensions calculated from linear viscoelsatic response using the analyses of Gramspacher and Messisner and Palierne agree reasonably with other estimates except near the phase inversion point. To study the effect of domain deformation, we measured G' and G'' at two different perturbation conditions. The magnitude of the strain amplitudes at low frequencies strongly affected G', presumably due to its sensitivity to the domain shape and size of the dispersed phase. The storage modulus also shows a frequency-dependent discontinuity where temperature is changed. Extrapolation of this frequency-dependent discontinuity temperature to zero frequency gives an estimate of T_C that agrees well with that determined from optical microscopy.

Acknowledgment. The authors thank Dr. Adel F. Halasa and Dr. Bill W. Hsu of The Goodyear Tire and Rubber Company for the synthesis of the polymers used in this study.

References and Notes

(1) Han, C. D. *Multiphase Flow in Polymer Processing*; Academic Press: New York, 1981.
(2) Utracki, L. A. *Polymer Alloys and Blends*; Hanser Publishers: New York, 1990.
(3) Min, K.; White, J. L.; Fetters, L. F. *J. Appl. Polym. Sci.* **1984**, *29*, 2117.
(4) Scholtz, P.; Froelich, D.; Muller, R. *J. Rheol.* **1989**, *33*, 481. Friedrich, Chr.; Gleinser, E.; Korat, E.; Maier, D.; Weese, J. *J. Rheol.* **1995**, *39*, 1411.
(5) Graebling, D.; Muller, R.; Palierne, J. F. *Macromolecules* **1993**, *26*, 320. Graebling, D.; Muller, R.; Palierne, J. F. *J. Phys. VI* **1993**, *3*, 1525.
(6) Gramespacher, H.; Meissner, J. *J. Rheol.* **1992**, *36*, 1127.
(7) Takahashi, Y.; Noda, I. In *Flow-Induced Structure in Polymers*; Nakatani, A. I., Dadmun, M. D., Eds.; American Chemical Society: Washington, DC, 1995. Kitade, S.; Ichikawa, A.; Imura, N.; Takahashi, Y. *J. Rheol.* **1997**, *41*, 1039.
(8) Kernick, W. A.; Wagner, N. J. *J. Rheol.* **1999**, *43*, 521. Minale, M.; Moldenaers, P.; Mewis, J. *J. Rheol.* **1999**, *43*, 815. Vinckier, I.; Minale, M.; Mewis, J.; Moldenaers, P. *Colloids Surf.* **1999**, *150*, 217. Vinckier, I.; Moldenaers, P.; Mewis, J. *J. Rheol.* **1996**, *40*, 613.
(9) Kitade, S.; Takahashi, Y.; Kitade, S.; Noda, I. *Macromolecules* **1994**, *27*, 7397. Takahashi, Y.; Suzuki, H.; Nakagawa, Y.; Noda, I. *Polym. Int.* **1994**, *34*, 327. Takahashi, Y.; Kitade. S.; Ochiai, K.; Noda, I. *Polym. J.* **1997**, *29*, 770.
(10) Ajji, A.; Choplin, L.; Prud'homme, R. E. *J. Polym. Sci., Part B: Polym. Phys.* **1988**, *26*, 2279. Mani, S.; Malone, M. F.; Winter, H. H.; Halary, J. L.; Monnerie, L. *Macromolecules* **1991**, *24*, 5451. Nesaricar, A. R. *Macromolecules* **1995**, *28*, 7202. Vlassopoulos, D. *Rheol. Acta* **1996**, *35*, 556. Mani, S.; Malone, M. F.; Winter, H. H. *J. Rheol.* **1992**, *36*, 1625.
(11) Pathak, J. A.; Colby, R. H.; Kamath, S. Y.; Kumar, S.; Stadler, R. *Macromolecules* **1998**, *31*, 8988.
(12) Palierne, J. F. *Rheol. Acta* **1990**, *29*, 204.
(13) Choi. S. J.; Schowalter, W. R. *Phys. Fluids* **1975**, *18*, 420.
(14) Valenza, A.; Lyngaae-Jorgensen, J.; Utracki, L. A.; Sammut, P. *Polym. Networks Blends* **1991**, *1*, 79.
(15) Jeon, H. S.; Nakatani, A. I.; Hsu, W.; Halasa, A. F.; Han, C. C. *ACS Polym. Mater.: Sci. Eng. Prepr.* **1999**, *80*, 349.
(16) The references to commercial equipment or materials do not imply recommendation or endorsement by the National Institute of Standard and Technology.
(17) According to ISO 31-8, the term molecular weight has been replaced by "relative molecular mass", M_r. The older, more conventional, notation for number-average (M_n) and weight-average (M_w) molecular weights is utilized in the present paper.
(18) Kim, S.; Yu, J. W.; Han, C. C. *Rev. Sci. Instrum.* **1996**, *67*, 3940.
(19) Brandrup, J.; Immergut, E. H. *Polymer Handbook*, 3rd ed.; Wiley-Interscience: New York, 1989; Chapter VI, p 455.
(20) Ferry, J. D. *Viscoelastic Properties of Polymers*, 2nd ed.; John Wiley and Sons: New York, 1970; p 44.
(21) Colby, R. H. *Polymer* **1989**, *30*, 1275. Zawada, J. A.; Fuller, G. G.; Colby, R. H.; Fetters, L. J.; Roovers, J. *Macromolecules* **1994**, *27*, 6851.
(22) Ajji, A.; Choplin, L.; Prud'homme, R. E. *J. Polym. Sci., Part B: Polym. Phys.* **1991**, *29*, 1573. Kapnistos, M.; Hinrichs, A.; Vlassopoulos, D.; Anastasiadis, S. H.; Stammer, A.; Wolf, B. A. *Macromolecules* **1996**, *29*, 7155.
(23) Vlassopoulos, D.; Koumoutsakos, A.; Anastasiadis, S. H.; Hatzikiriakos, S. G.; Englezos, P. *J. Rheol.* **1992**, *41*, 739. Kapnistos, M.; Vlassopoulos, D.; Anastasiadis, S. H. *Europhys. Lett.* **1996**, *34*, 513.
(24) To confirm characteristics of the equilibrium compositions of PB/PI blends as a function of temperature, we determined the order parameter exponent β from a power-law fit of the composition difference $\Delta\phi$ as a function of reduced temperature, $\tau = (T - T_C)/T_C$, leading to the relation $\Delta\phi_{PI}(T) = 0.89\tau^{\beta}$ with $\beta = 0.350 \pm 0.002$. The β value determined from the power-law fit is intermediate between the Ising value ($\beta \approx 0.326$) and the fully Fisher-normalized value ($\beta \approx 0.366$) and identical to the value ($\beta = 0.35 \pm 0.01$) of PB/PS blend [see ref 32].
(25) Jeon, H. S.; Nakatani, A. I.; Han, C. C. *ACS Polym. Mater.: Sci. Eng. Prepr.* **2000**, *82*, 85.
(26) Taylor, G. I. *Proc. R. Soc. London A* **1934**, *146*, 501.
(27) Broseta, D.; Fredrickson, G. H.; Helfand, E.; Leibler, L. *Macromolecules* **1990**, *23*, 132.
(28) Balsara, N. P. In *Physical Properties of Polymer Handbook*; AIP Press: Woodbury, NY, 1996; Chapter 19, p 257.
(29) The parameters used in the calculation of the interfacial tension of PB/PI blend are given by $\chi = 0.00468 - 1.01/T$ with a reference volume of 111.5 Å^3, $\rho_0 = (\rho_{PB}\rho_{PI})^{1/2}$ with $\rho_{PB} = 0.0097$ Å^{-3} and $\rho_{PI} = 0.0078$ Å^{-3}, $b = (b_{PB}b_{PI})^{1/2}$ with $b_{PB} = 9.2$ Å and $b_{PI} = 9.2$ Å, $N_{PB} = 943$, and $N_{PI} = 1292$ at 130 °C.
(30) Utracki, L. A. *J. Rheol.* **1991**, *35*, 1615.
(31) Grizzuti, N.; Buonocore, G.; Iorio, G. *J. Rheol.* **2000**, *44*, 149.
(32) Yu, J. W.; Douglas, J. F.; Hobbie, E. K.; Kim, S.; Han, C. C. *Phys. Rev. Lett.* **1997**, *78*, 2664.

MA000714U